

MgO/Ag(100): Confined vibrational modes in the limit of ultrathin films

L. Savio,* E. Celasco, L. Vattuone, and M. Rocca

Istituto Nazionale di Fisica della Materia, Unita' di Genova and IMEM-CNR, Dipartimento di Fisica, Universtit  di Genova, Via Dodecaneso 33, 16146 Genova, Italy

P. Senet

CNRS UMR 5027, Laboratoire de Physique, Th orie de la Mati re Condens e, Universit  de Bourgogne, 9 Avenue Alain Savary, B.P. 47870, F-21078 Dijon Cedex, France

(Received 22 July 2002; published 28 February 2003)

The vibrational modes of clean MgO films are investigated vs film thickness by means of high-resolution electron energy-loss spectroscopy. For thin films (20–30 monolayers) we observe, in accord with the literature, the Fuchs-Kliewer phonon at 677 cm^{-1} and the Wallis mode at 524 cm^{-1} . For ultrathin films standing wave optical phonons confined in the overlayer are present, whose frequencies depend strongly on film thickness. Comparison with theoretical calculations for MgO slabs on a perfect conductor shows that the experimental frequencies are lower than expected, indicating the presence of compressive stress. At and below one-monolayer thickness an intense loss peak at 427 cm^{-1} is observed.

DOI: 10.1103/PhysRevB.67.075420

PACS number(s): 68.35.Ja, 81.15.-z

I. INTRODUCTION

The wide interest in magnesium oxide originates from its technological applications as well as from its role as a model system for the investigation of metal oxides. For these reasons the system was thoroughly studied in the past years both theoretically and experimentally, although most of the attention was devoted, until now, to thin films or to bulk MgO.^{1–5} The main feature observed in spectroscopic investigations performed by high-resolution electron energy-loss spectroscopy (HREELS) is the Fuchs-Kliewer (FK) mode,⁷ a macroscopic surface optical phonon, corresponding to the vibration of the Mg and O sublattices one against the other. According to dielectric continuum theory⁸ this mode is expected at the frequency

$$\omega_{FK} = \omega_{TO} \sqrt{\frac{\epsilon_{\infty} + 1}{\epsilon_0 + 1}}, \quad (1)$$

where ω_{TO} is the frequency of the bulk transverse-optical phonon and ϵ_0 and ϵ_{∞} are the static and high-frequency dielectric constants, respectively. For bulk MgO, for which $\epsilon_0 = 9.8$, $\epsilon_{\infty} = 2.95$, and $\omega_{TO} = 393\text{ cm}^{-1}$,^{9,10} ω_{FK} is expected at 649.6 cm^{-1} from Eq. (1), in agreement with the measured value of 650.4 cm^{-1} for MgO(100).^{4,5} In addition to the FK optical phonon predicted by macroscopic theory, the surface microscopic phonon S_2 (Wallis mode) was reported at 524 cm^{-1} .⁵ This mode corresponds to the microscopic perpendicular motion of oxygen atoms in the topmost layer.

For an insulating film of thickness d on a substrate which has no infrared-active modes, dielectric continuum theory predicts the presence of two dipolar active modes, FK^+ and FK^- , whose evanescent electric fields extend at a distance $\approx 1/Q$, where Q is the phonon wave vector parallel to the surface.^{7,11} If $d \gg 1/Q$, these two macroscopic optical modes are well separated in space and correspond to large vibrations of the atoms at the surface and at the interface of the

film for FK^+ and FK^- , respectively. If $d \ll 1/Q$, on the contrary, all the atoms in the film are involved in the motion due to the FK modes, both in the directions parallel or normal to the surface. Their behavior becomes more complex and depends on thickness.^{12,13} In the case where the substrate is a perfect metal, the FK^- mode is completely screened and cannot be observed.

For films grown by oxidizing Mg single crystals the FK^+ phonon energy was found to increase with oxygen exposure from 620 cm^{-1} to 658 cm^{-1} .¹⁴ For a 2-monolayer (ML) MgO film, supported on TiC(100), on the contrary, the FK^+ mode was reported at 693 cm^{-1} ,¹⁵ while the Wallis mode is at 524 cm^{-1} , as for bulk MgO(100).⁵

Thin and ultrathin oxide films are of current interest because of their possible electronic applications, e.g., their employment in the construction of nanodevices, magnetic tunnel junctions, or insulating barriers for miniaturized electronic devices. Moreover, contrary to bulk crystals or thick films, they can easily be investigated with electronic spectroscopies. Their structure and electronic properties are still poorly known and might be significantly different from those of thick films. Moreover it was recently shown that the vibrational modes of thin and ultrathin oxide films are sensitive to the presence of adsorbates.⁶

Ag(100) is a good template for the growth of MgO layers since the lattice mismatch is 4%, leading to only slightly compressed oxide films. A spot profile analysis low-energy electron-diffraction investigation on a 6.5-ML film at 350 K (Refs. 16 and 17) showed the presence of a mosaic structure formed by flat and slightly tilted grains some tens of nm large. More recently it was shown by scanning-tunneling microscopy (STM) that MgO initially forms two-dimensional square islands homogeneously distributed on the surface. After deposition of 2 ML of MgO the substrate is completely covered and the film consists of terraces, typically 50-nm wide, and of three-dimensional pyramids.¹⁸ Other STM experiments¹⁹ showed that, at 1 ML of nominal coverage, approximately 60% of the substrate surface is covered by a

single MgO layer, while 25% consists of MgO pyramids, and the remaining part is still bare.

In the present paper we report on the behavior of surface phonons vs film thickness for MgO films from 0.3 ML to 30 ML, grown on Ag(100). We observe the FK^+ mode at $572\text{--}677\text{ cm}^{-1}$, depending on film thickness, and the microscopic mode at 524 cm^{-1} . A further intense mode is observed at 427 cm^{-1} in the monolayer and submonolayer limits. The data are compared with microscopic calculations of HREEL spectra for MgO films on a metal,²⁰ which show the presence of optical standing waves confined in the film.¹²

II. EXPERIMENTAL AND THEORETICAL METHODS

Experiments were carried out in an ultrahigh vacuum (UHV) apparatus equipped with a Knudsen cell for Mg evaporation, a quartz microbalance for Mg flux measurements, a commercial HREEL spectrometer (SPECS Instruments), and all other typical vacuum facilities. The substrate was an Ag single crystal cut within 0.1° from the (100) plane, which was carefully cleaned by sputtering and annealing to 720 K before each experiment. Several cycles were repeated until the surface was completely clean, i.e., no loss features were detected in the HREEL spectra. MgO films were grown by reactive deposition at a crystal temperature $T=453\text{ K}$. To reduce the presence of contaminants, a doser, placed at 1.5 cm from the Ag(100) surface, was employed to expose O_2 during Mg evaporation. The background pressure, therefore, did not exceed 3.10^{-8} mbar during the growth process, while the O_2 partial pressure at the surface was about 10 times larger. The film thickness was evaluated by calibration of the Mg flux through the quartz microbalance and by the analysis of the FK mode intensities. HREEL spectra were recorded in-specularly, at an angle of incidence of 60° and at a primary electron energy, E_e , of 3 or 4 eV. The typically achieved energy resolution was 4.0 meV. The angular acceptance of the spectrometer was $\Delta\theta=1^\circ$ and corresponded to integrating over $\approx 0.008\text{ \AA}^{-1}$ in reciprocal space in our experimental conditions. The integration window was thus comparable with the wave-vector transfer for our in-specular measurements.

Theoretical HREEL spectra can be computed from the surface dielectric response $g(Q,\omega)$ which has poles at the dipolar active modes.^{11,21,22} In dielectric continuum theory, g is computed from the dielectric functions of the MgO film and of the metal substrate and has only two poles at the frequencies of the FK^+ and FK^- modes.¹¹ This macroscopic approach is only valid for a thickness larger than about 3 nm.¹² For thinner films g must be evaluated from a microscopic theory based on lattice dynamics.^{23,24} The microscopic response g has poles at the frequencies of the optical LO and TO modes of the film, building the FK macroscopic phonons, and at the frequencies of some microscopic surface phonons, not included in the dielectric continuum approach.²⁵ In the present work, we applied the microscopic approach to the MgO thin layers grown on a metal. The layers were modeled by MgO(001) slabs on a perfect conductor.^{20,24} The dynamics of the ions was described by a shell model which reproduces the bulk phonon-dispersion

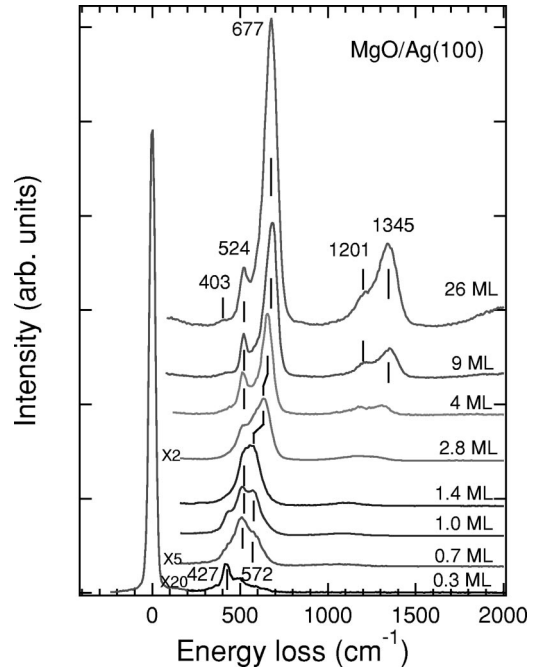


FIG. 1. Experimental HREEL spectra of clean MgO films of different thicknesses. All the spectra were recorded in-specularly at an angle of incidence of 60° with $E_e=4.0\text{ eV}$, except for the two upper ones, for which $E_e=3.0\text{ eV}$. Three losses are visible corresponding to the FK^+ mode and to two microscopic modes.

curves measured by neutron scattering.²⁶ The geometry of the film on the metal was relaxed using this shell model according to the procedure described in Ref. 27.

III. RESULTS

Figure 1 shows the vibrational spectra of clean MgO films of different thicknesses. All the spectra are recorded in-specularly with $E_e=4.0\text{ eV}$, except for the two upper ones, for which $E_e=3.0\text{ eV}$. Several peaks are present in the range between 400 cm^{-1} and 700 cm^{-1} , the position and the intensity of which depends strongly on film thickness. The spectrum relative to the 26-ML film ($d=5.5\text{ nm}$, upper curve) is dominated by a strong feature at 675 cm^{-1} , with a minor peak at 524 cm^{-1} . The high-frequency feature is the FK^+ macroscopic phonon, and the 524-cm^{-1} peak is assigned to the microscopic Wallis mode. A further, very weak, loss is present at 400 cm^{-1} only for the largest thickness. We have no explanation for it since its frequency might be indicative of the excitation of the FK mode (expected at about 395 cm^{-1} in MgO), which is, however, not expected to be dipole active. The feature at 1201 cm^{-1} results from the combination loss of the FK^+ and Wallis modes; the one at 1354 cm^{-1} , on the contrary, is the FK^- double loss. The intensity of combined and double losses becomes negligible for thinner films on this scale. We note that, in principle, comparing spectra recorded at different E_e is not correct since they correspond to different values of parallel momentum transfer. The measurements are, however, mediated over an angular acceptance of 1° which corresponds to an integration in reciprocal space comparable to the nominal wave-

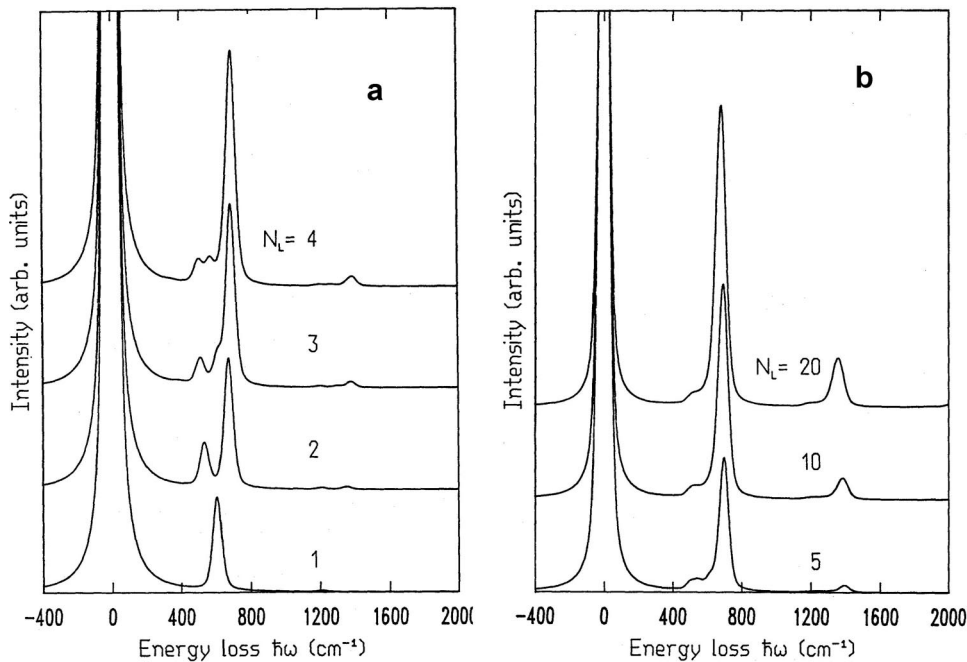


FIG. 2. Theoretical HREEL spectra calculated for a relaxed MgO(100) slab of 1 to 4 ML (a) and of 5 to 20 ML (b). Calculations were performed for a primary electron energy of 6.0 eV and an angle of incidence of the electrons of 45° .

vector transfer (of the order of 0.008 \AA^{-1} at $E_e = 4.0 \text{ eV}$). In accord with this no difference in the loss peak positions was observed when varying E_e between 3.0 and 6.0 eV.

When decreasing the film thickness, the energy of the FK^+ mode shifts towards lower values, reading 572 cm^{-1} at 1 ML ($d = 0.21 \text{ nm}$). A similar behavior was reported by Gao *et al.*¹³ for LiBr/Si(100) and by Liehr *et al.* for $\text{CaF}_2/\text{Si}(111)$.²⁸ The Wallis mode is present for all film thicknesses, its energy shifting from 524 cm^{-1} to 508 cm^{-1} when the coverage becomes 1 ML or less. In the monolayer and submonolayer regimes a third peak grows at 427 cm^{-1} , whose relative intensity becomes dominant for the 0.3-ML film.

The results of the microscopic calculations of the HREEL spectrum using $g(Q, \omega)$ for MgO slabs from 1-ML-to-20-ML thicknesses deposited on a perfect conductor are reported in Figs. 2(a) and 2(b) for $E_e = 6 \text{ eV}$ and $\theta = 60^\circ$. Theory describes quite fairly the *increase* of the loss energy of the macroscopic phonon FK^+ with film thickness, but fails in reproducing its exact energy, the measured values being systematically lower than theory. The wave-vector transfer in theory is slightly different than in experiment but again the difference is well within the experimental integration window in reciprocal space so that the discrepancy cannot be due to phonon dispersion with Q .

The experimental results for all losses are collected in Fig. 3 and compared with the result of theory for the FK^+ frequency. Closed symbols refer to experiment [FK^+ mode (\circ), Wallis mode (\diamond), and monolayer mode (\square)], and open symbols to theory (the FK^+ mode is calculated within the microscopic approach previously described [open (\circ)] and within dielectric continuum theory [crossed circles]). For the largest thickness both theories describe the decrease of the loss energy, which reaches eventually the bulk value of 650 cm^{-1} . This effect is analogous to the LiBr/Si(111) case.¹² The initial increase of the FK^+ energy with thickness,

on the contrary, is reproduced only by the microscopic theory. In addition, it predicts a contribution of *several* modes at frequencies lower than the FK^+ phonon, which results in a weak, nondispersive peak around 550 cm^{-1} . The latter peak coincides with the Wallis mode at 524 cm^{-1} in the thick-film limit. No dipolar active mode around 400 cm^{-1} is found in the simulations, for which perfect screening of the metal substrate was assumed. Theory systematically overestimates the FK^+ phonon frequencies, the discrepancy being larger for thinner films.

IV. DISCUSSION

The long-wavelength phonon spectrum of ultrathin films can be very well described by standing waves confined in the

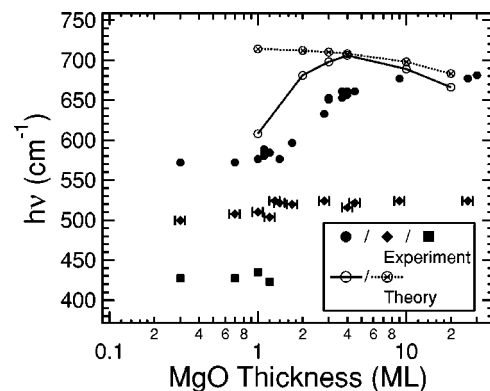


FIG. 3. MgO vibrational frequencies as a function of film thickness. The filled symbols refer to the experimentally observed modes: FK^+ (closed \circ), Wallis (\diamond), and 427-cm^{-1} vibration (\square). The error for film thickness is estimated to be $\pm 8\%$. The open circles refer to the theoretical values for the FK^+ mode calculated using the microscopic approach described in the text. The crossed circles refer, on the contrary, to the forecasts within dielectric continuum theory.

film as observed for longitudinal-acoustical modes in Na/Cu(001) by helium atom scattering²⁹ and for longitudinal and optical modes in LiBr/Si(111) by HREELS.^{12,13} The frequency of the standing waves corresponds approximately to those of bulk phonons at wave vectors $(0,0,q_z)$ in which q_z is an effective wave vector in the normal direction to the surface, which is quantized due to the finite film thickness and to the reflection of the waves by the substrate. For MgO/Ag(100) we expect the presence of a node for the outermost substrate layer, which cannot follow the relatively large frequency of the MgO phonons, and either a node or a maximum at the MgO surface layer. In these conditions, for a MgO film of N_L -monolayers thickness on a perfect conductor, the effective wave vector of the optical standing waves LO_n and TO_n are given, respectively, by the following quantization rules:

$$q_z = \frac{(2n-1)\pi}{N_L a}, \quad (2)$$

$$q_z = \frac{2n\pi}{N_L a}, \quad (3)$$

where N_L is the number of MgO layers, n is an integer ($1 \leq n \leq N_L$), and $a = 4.21 \text{ \AA}$ is the lattice parameter (1 ML corresponds thus to a thickness of $a/2$), with the condition that at least one atom of the film does not coincide with a node. We note that the substrate modifies only the frequencies of LO modes compared to those of the corresponding modes of an isolated slab. The frequencies of the standing waves can then be recovered from the bulk dispersion curves measured for MgO in the Γ -X direction by applying Eqs. (2) and (3). This procedure yields, e.g., a triplet for the LO phonons, at $\omega_{LO_1} = 707 \text{ cm}^{-1}$, $\omega_{LO_2} = 629 \text{ cm}^{-1}$, and $\omega_{LO_3} = 548 \text{ cm}^{-1}$, for $N_L = 3$ ML.

In a macroscopic theory, the frequency of the FK^+ phonon for $Qd \rightarrow 0$ is ω_{LO} .⁸ However for thin films ($d \rightarrow 0$) several LO_n modes are expected. It has been demonstrated that the phonon with the highest intensity detected by HREELS in thin films, FK^+ , is in fact the LO mode with the largest wavelength in the direction perpendicular to the film, i.e., corresponding to LO_1 .¹² Because the bulk phonon frequency $\omega_{LO}(q_z)$ in the Γ -X direction for MgO decreases when k_z approaches the boundary of the Brillouin zone, as for many ionic crystals,³⁰ the frequency $\omega_{LO_1} = \omega_{LO}(\pi/N_L a)$ increases with N_L , as shown both by experiment and theory in Fig. 3.

For a small number of layers, the other LO_n modes also contribute to the dipolar response with a weight rapidly decreasing with thickness. This explains the features on the left of the FK^+ peak in Figs. 1 and 2. At larger thickness, $Qd \gg 1$, macroscopic theory predicts a dispersive phonon FK^+ which is microscopically built from several LO_n at different wave vectors.²³ In Fig. 3, one observes in addition to the FK^+ mode the contribution of the LO_{N_L} mode. We note that in lattice dynamics calculations of ionic films this mode is not, in general, a simple projection of the corresponding bulk mode but behaves as a surface microscopic phonon. This is

because it has the shortest wavelength perpendicular to the film and is therefore strongly perturbed by the creation of the surface. In the largest MgO films studied here, we can clearly identify this mode as the S_2 or Wallis mode.

Interestingly the experiment shows a shift of its frequency when crossing the 1-ML threshold. We believe that this effect corresponds to the different vibrational energy of oxygen atoms vibrating against the Ag substrate instead of against underlying MgO layers.

The calculations deal with an ideal film/substrate system in which the bonds between the film and the substrate are taken into account with a simple image method.²⁴ The effect of the compressive stress in the film, caused by the 0.12-\AA difference between the MgO and the Ag lattice spacings of the fcc unit cell, as well as possible changes in the force constants, were not taken into account. We believe that compressive stress in the film is the most probable cause for the reduction of the phonon frequencies in the ultrathin-film limit.

More interestingly, theory does not reproduce the contribution at 427 cm^{-1} found experimentally in the submonolayer regime. This mode could have three possible origins: (i) it might be due to the vibration of the whole film against the substrate, (ii) it might be due to the excitation of the optical vibration of the MgO layer parallel to the surface, or (iii) it might be associated with the microscopic vibration of oxygen atoms with lower coordination than terrace atoms. Hypothesis (i) is improbable since we would expect a lower frequency for this mode. Hypothesis (ii) is also unlikely, although according to theory¹² the frequency of such vibration should be equal to the one of the TO_1 mode, i.e., at about 445 cm^{-1} as deduced from the neutron-scattering data using Eq. (3) with $N_L = 1$ ML; we reject this possibility since this mode is not totally symmetric and thus cannot be dipole active.

Hypothesis (iii) is in our opinion the most likely. Less coordinated oxygen can be found, e.g., at the edge of MgO islands (threefold coordinated) or at their corners (twofold coordinated). At the lowest coverage the fraction of such low coordinated oxygen is indeed expected to exceed the one of the fourfold coordinated ones inside the islands. Indeed the ratio $427/508$ nearly coincides with the square root of $3/4$, i.e., with the ratio of the coordination numbers of oxygen in the film and at edge sites. We stress on the other hand that no loss at 427 cm^{-1} is observed for multilayers, although because of the nonuniformity of such films, steps are expected to be abundant also in that case. One further possibility is, however, that oxygen atoms at steps of multilayer films vibrate at 403 cm^{-1} , thus explaining the feature observed experimentally in the thin-film limit.

We notice finally that the ratio of the intensity of the peaks at 427 cm^{-1} and 508 cm^{-1} could be controlled only over a factor of 2 for films of the same nominal coverage. If the loss at 427 cm^{-1} was due to edge oxygen atoms, this would mean that shape and size of the MgO islands could depend critically on some poorly controlled parameter during film growth.

V. CONCLUSION

In conclusion we have measured the energy-loss spectrum of thin and ultrathin MgO films and compared the frequency of the detected modes with theoretical predictions. HREEL spectra of ultrathin films are dominated by optical standing waves, as already reported for LiBr/Si(100).^{12,13} The FK mode sets in eventually and shifts with thickness. The imperfect match between experiment and theory is indicative of

the presence of compressive stress. A mode at 427 cm^{-1} is present for the monolayer and submonolayer regimes, which might be due to less coordinated oxygen atoms.

ACKNOWLEDGMENTS

We acknowledge financial support from INFM PRA ISA-DORA and MIUR PRIN Project No. 2001023192.

*Present address: Institut für Experimentalphysik, Freie Universität-Berlin, Arnimalle 14, Berlin (Germany).

¹H. Ibach, Phys. Rev. Lett. **24**, 1416 (1970).

²D.W. Goodman, J. Vac. Sci. Technol. A **14**, 1526 (1996).

³A. Kolmakov, J. Stultz, and D.W. Goodman, J. Chem. Phys. **113**, 7564 (2000).

⁴P.A. Thiry, M. Liehr, J.J. Pireaux, and R. Caudano, Phys. Rev. B **29**, 4824 (1984).

⁵C. Oshima, T. Aizawa, R. Souda, and Y. Ishizawa, Solid State Commun. **73**, 731 (1990).

⁶M. Frank, K. Wolter, N. Magg, M. Heemeir, R. Kühnemuth, M. Bäumer, and H.J. Freund, Surf. Sci. **492**, 270 (2001).

⁷R. Fuchs and K.L. Kliewer, Phys. Rev. **150**, 573 (1966).

⁸H. Froitzheim, H. Ibach, and D.L. Mills, Phys. Rev. B **11**, 4980 (1975).

⁹T. Gourtley and W.A. Runciman, J. Phys. C **6**, 583 (1973).

¹⁰S. Nagel, K. Maschke, and A. Baldereschi, Phys. Status Solidi B **76**, 629 (1976).

¹¹H. Ibach and D.L. Mills, *Electron Energy Loss Spectroscopy and Surface Vibrations* (Academic, New York, 1982).

¹²P. Senet, Ph. Lambin, and A.A. Lucas, Phys. Rev. Lett. **74**, 570 (1995).

¹³W. Gao, Y. Fujikawa, K. Saiki, and A. Koma, Solid State Commun. **87**, 1013 (1993).

¹⁴P.A. Thiry, J. Ghijsen, R. Sporcken, J.J. Pireaux, R.L. Johnson, and R. Caudano, Phys. Rev. B **39**, 3620 (1989).

¹⁵Y. Hwang, R. Souda, T. Aizawa, W. Hayami, S. Otani, and Y. Ishizawa, Jpn. J. Appl. Phys., Part 1 **36**, 5707 (1997).

¹⁶J. Wollschläger, D. Erdos, and K.M. Schroder, Surf. Sci. **402/404**,

272 (1998).

¹⁷J. Wollschläger, D. Erdos, H. Goldbach, and K.M. Schroder, Thin Solid Films **400**, 1 (2001).

¹⁸S. Schintke, S. Messerli, M. Pivetta, F. Patthey, L. Libioulle, M. Stengel, A. De Vita, and W.-D. Schneider, Phys. Rev. Lett. **87**, 276801 (2001).

¹⁹S. Valeri, S. Altieri, U. Del Pennino, A. Di Bona, P. Luches, and A. Rota, Phys. Rev. B **65**, 245410 (2002).

²⁰P. Senet, Ph.D. thesis, University of Namur, 1993.

²¹A.A. Lucas and M. Sunjic, Phys. Rev. Lett. **26**, 229 (1971).

²²Ph. Lambin, J.P. Vigneron, and A.A. Lucas, Comput. Phys. Commun. **60**, 351 (1990).

²³P. Senet, Ph. Lambin, J.-P. Vigneron, I. Derycke, and A.A. Lucas, Surf. Sci. **226**, 307 (1990).

²⁴Ph. Lambin, P. Senet, and A.A. Lucas, Phys. Rev. B **44**, 6416 (1991).

²⁵P. Senet, Ph. Lambin, and A.A. Lucas, Surf. Sci. **269/270**, 141 (1992).

²⁶M.J.L. Sangster, G. Peckham, and D.M. Saunderson, J. Phys. C **3**, 1026 (1970), model B.

²⁷F.W. de Wette, W. Kress, and U. Schröder, Phys. Rev. B **32**, 4143 (1985).

²⁸M. Liehr, P.A. Thiry, J.J. Pireaux, and R. Caudano, Phys. Rev. B **34**, 7471 (1986).

²⁹G. Benedek, J. Ellis, A. Reichmuth, P. Ruggerone, H. Schief, and J.P. Toennies, Phys. Rev. Lett. **69**, 2951 (1992).

³⁰H. Biltz and W. Kress, *Phonon Dispersion Relations in Insulators*, Springer Series in Solid State Science, Vol. 10 (Springer, New York, 1991).